

## Semileptonic weak decays of antitriplet charmed baryons in the light-front formalism

C. Q. Geng,<sup>1,2,3</sup> Chia-Wei Liu,<sup>1,2,3</sup> and Tien-Hsueh Tsai<sup>3</sup>

<sup>1</sup>*School of Fundamental Physics and Mathematical Sciences, Hangzhou Institute for Advanced Study, UCAS, Hangzhou 310024, China*

<sup>2</sup>*International Centre for Theoretical Physics Asia-Pacific, Beijing/Hangzhou, China*

<sup>3</sup>*Department of Physics, National Tsing Hua University, Hsinchu 300, Taiwan*



(Received 15 January 2021; accepted 3 March 2021; published 18 March 2021)

We systematically study the semileptonic decays of  $\mathbf{B}_c \rightarrow \mathbf{B}_n \ell^+ \nu_\ell$  in the light-front constituent quark model, where  $\mathbf{B}_c$  represents the antitriplet charmed baryons of  $(\Xi_c^0, \Xi_c^+, \Lambda_c^+)$  and  $\mathbf{B}_n$  corresponds to the octet ones. We determine the spin-flavor structures of the constituents in the baryons with the Fermi statistics and calculate the decay branching ratios ( $\mathcal{B}$ s) and averaged asymmetry parameters ( $\alpha$ s) with the helicity formalism. In particular, we find that  $\mathcal{B}(\Lambda_c^+ \rightarrow \Lambda e^+ \nu_e, n e^+ \nu_e) = (3.55 \pm 1.04, 0.36 \pm 0.15)\%$ ,  $\mathcal{B}(\Xi_c^+ \rightarrow \Xi^0 e^+ \nu_e, \Sigma^0 e^+ \nu_e, \Lambda e^+ \nu_e) = (11.3 \pm 3.35), 0.33 \pm 0.09, 0.12 \pm 0.04\%$ , and  $\mathcal{B}(\Xi_c^0 \rightarrow \Xi^- e^+ \nu_e, \Sigma^- e^+ \nu_e) = (3.49 \pm 0.95, 0.22 \pm 0.06)\%$ . Our results agree with the current experimental data. Our prediction for  $\mathcal{B}(\Lambda_c^+ \rightarrow n e^+ \nu_e)$  is consistent with those in the literature, which can be measured by the charm facilities, such as BESIII and BELLE. Some of our results for the  $\Xi_c^{+(0)}$  semileptonic channels can be tested by the experiments at BELLE as well as the ongoing ones at LHCb and BELLEII.

DOI: [10.1103/PhysRevD.103.054018](https://doi.org/10.1103/PhysRevD.103.054018)

### I. INTRODUCTION

In the recent few years, there have been two important experiments in charmed baryon physics. One is the measurement of the absolute branching ratios of  $\mathcal{B}(\Xi_c^0 \rightarrow \Xi^- \pi^+) = (1.8 \pm 0.5)\%$  [1] and  $\mathcal{B}(\Xi_c^+ \rightarrow \Xi^- \pi^+ \pi^+) = (2.86 \pm 1.21 \pm 0.38)\%$  [2] from the Belle Collaboration, and the other is the most precise measurement of the  $\Xi_c^0$ 's lifetime of  $\tau_{\Xi_c^0} = 154.5 \pm 1.7 \pm 1.6 \pm 1.0$  fs from the LHCb Collaboration [3], which significantly deviates from the past world averaged value of  $\tau_{\Xi_c^0} = 112_{-10}^{+13}$  fs in PDG [4]. Both of them bring us new hints as well as new problems in charm physics. We are now in a precision era of charm physics. It is expected that as more high quality data will be accumulated in the future, stronger constraints on various baryonic QCD models as well as physics beyond the standard model can be given.

Recently, the antitriplet charm baryon decays have been extensively discussed in the literature. However, due to the large nonperturbative effects from the quantum chromodynamics (QCD), the decay amplitudes and observables of hadrons are very hard to obtain from the QCD first principle. To avoid the difficulties, various charmed baryon

decay processes have been studied based on the flavor symmetry of  $SU(3)_f$ , such as semileptonic, two-body, and three-body nonleptonic decays, to get reliable results [5–24]. It is known that  $SU(3)_f$  is an approximate symmetry, resulting in about 10% of uncertainties for the predictions inherently. Moreover, the  $SU(3)_f$  symmetry itself does not directly reveal any clue about the QCD dynamics. In fact, its applications heavily rely on the experimental data as inputs. In order to have precise calculations, we need a specific dynamical QCD model to understand each decay process. For simplicity, we only discuss the semileptonic processes of the antitriplet charmed baryons in this study, which involve purely factorizable contributions. There are several theoretical calculations on these decay processes with different QCD frameworks in the literature [25–34].

The light front (LF) QCD formalism in the quark model is a consistent relativistic approach, which has been tested successfully in the mesonic and light quark sectors in early times [35,36]. Because of these successes, it has been used in other generalized systems, such as those containing the heavy mesons, pentaquarks, and so on [37–44]. Apart from the charm system, the bottom to charmed baryon nonleptonic decays have been recently analyzed in the LF formalism [45]. For a review on the comprehensive introduction of the LF QCD and its vacuum structure, one can refer to Ref. [35]. For the LF constituent quark model (LFCQM), we recommend Ref. [36] and references therein. The advantage of LFCQM is that we can boost the reference frame without changing the equation of motion

Published by the American Physical Society under the terms of the [Creative Commons Attribution 4.0 International license](https://creativecommons.org/licenses/by/4.0/). Further distribution of this work must maintain attribution to the author(s) and the published article's title, journal citation, and DOI. Funded by SCOAP<sup>3</sup>.

because of the commutativity of the LF Hamiltonian and boost generators. It provides us with a great convenience to calculate the wave function in different inertial frames because of the recoil effects in the transition form factors.

This paper is organized as follows. We first present our formal calculations of the branching ratios and averaged decay asymmetries in terms of the helicity amplitudes, the baryonic states in LFCQM, and the baryonic transition form factors in Sec. II. In Sec. III, we show our numerical results and compare them with those in the literature. In Sec. IV, we give our conclusions.

## II. FORMALISM

### A. Helicity amplitudes and observables

The effective Hamiltonian for the antitriplet charmed baryon semileptonic weak decays can be written as

$$\mathcal{H}_{\text{eff}} = \frac{G_F}{\sqrt{2}} V_{cq} (\bar{\nu}_\ell \ell)_{V-A} (\bar{q}c)_{V-A}, \quad (1)$$

where  $G_F$  is the Fermi constant,  $V_{cq}$  is the CKM matrix element, and  $(\bar{\nu}_\ell \ell)_{V-A}$  and  $(\bar{q}c)_{V-A}$  denote the usual  $V - A$  currents  $\bar{\ell}\gamma^\mu(1 - \gamma_5)\nu_\ell$  and  $\bar{q}\gamma_\mu(1 - \gamma_5)c$  with  $q = d, s$ , respectively. The weak transition amplitudes of the antitriplet charmed baryons are given by

$$\begin{aligned} & A(\mathbf{B}_c \rightarrow \mathbf{B}_n \ell^+ \nu_\ell) \\ &= \frac{G_F}{\sqrt{2}} V_{cq} \bar{\ell}\gamma^\mu(1 - \gamma_5)\nu_\ell \langle \mathbf{B}_n | \bar{q}\gamma_\mu(1 - \gamma_5)c | \mathbf{B}_c \rangle, \end{aligned} \quad (2)$$

where the baryon transition matrix elements are parametrized by

$$\begin{aligned} & \langle \mathbf{B}_n, p_f, S'_z | \bar{q}\gamma_\mu(1 - \gamma_5)c | \mathbf{B}_c, p_i, S_z \rangle \\ &= \bar{u}_{\mathbf{B}_n}(p_f, S'_z) \left[ \gamma_\mu f_1(k^2) - i\sigma_{\mu\nu} \frac{k^\nu}{M_{\mathbf{B}_c}} f_2(k^2) + f_3(k^2) \frac{k_\mu}{M_{\mathbf{B}_c}} \right] \\ & \quad \times u_{\mathbf{B}_c}(p_i, S_z) \\ & - \bar{u}_{\mathbf{B}_n}(p_f, S'_z) \left[ \gamma_\mu g_1(k^2) - i\sigma_{\mu\nu} \frac{k^\nu}{M_{\mathbf{B}_c}} g_2(k^2) + g_3(k^2) \frac{k_\mu}{M_{\mathbf{B}_c}} \right] \\ & \quad \times \gamma_5 u_{\mathbf{B}_c}(p_i, S_z), \end{aligned} \quad (3)$$

with  $k^\mu = p_i^\mu - p_f^\mu$ ,  $\sigma_{\mu\nu} = \frac{i}{2}[\gamma_\mu, \gamma_\nu]$ , and  $f_i(k^2)$  and  $g_i(k^2)$  being the form factors describing the nonperturbative QCD effect in the timelike range of  $m_\ell^2 < k^2 < (M_{\mathbf{B}_c} - M_{\mathbf{B}_n})^2$ .

We introduce a set of helicity amplitudes  $H_{\lambda_2 \lambda_W}^{V(A)}$  to calculate the decay branching ratios and other physical quantities, where  $\lambda_2$  and  $\lambda_W$  represent the helicity quantum numbers of the daughter baryon and off shell  $W^+$  boson in the decay processes, respectively. These amplitudes give more intuitive physical pictures about the helicity structures of the decay processes. Furthermore, when we evaluate the asymmetries of these processes, such as the integrated (averaged) decay asymmetry, also known as the longitudinal polarization of the daughter baryon, these amplitudes result in much simpler expressions than the traditional ones. Relations between the helicity amplitudes and form factors are given by [33,46]

$$\begin{aligned} H_{\frac{1}{2}1}^V &= \sqrt{2K_-} \left( -f_1(k^2) - \frac{M_{\mathbf{B}_c} + M_{\mathbf{B}_n}}{M_{\mathbf{B}_c}} f_2(k^2) \right), \\ H_{\frac{3}{2}0}^V &= \frac{\sqrt{K_-}}{\sqrt{k^2}} \left( (M_{\mathbf{B}_c} + M_{\mathbf{B}_n}) f_1(k^2) + \frac{k^2}{M_{\mathbf{B}_c}} f_2(k^2) \right), \\ H_{\frac{1}{2}1}^V &= \frac{\sqrt{K_+}}{\sqrt{k^2}} \left( (M_{\mathbf{B}_c} + M_{\mathbf{B}_n}) f_1(k^2) + \frac{k^2}{M_{\mathbf{B}_c}} f_3(k^2) \right), \\ H_{\frac{1}{2}1}^A &= \sqrt{2K_+} \left( -g_1(k^2) - \frac{M_{\mathbf{B}_c} + M_{\mathbf{B}_n}}{M_{\mathbf{B}_c}} g_2(k^2) \right), \\ H_{\frac{3}{2}0}^A &= \frac{\sqrt{K_+}}{\sqrt{k^2}} \left( (M_{\mathbf{B}_c} - M_{\mathbf{B}_n}) g_1(k^2) - \frac{k^2}{M_{\mathbf{B}_c}} g_2(k^2) \right), \\ H_{\frac{1}{2}1}^A &= \frac{\sqrt{K_-}}{\sqrt{k^2}} \left( (M_{\mathbf{B}_c} - M_{\mathbf{B}_n}) g_1(k^2) - \frac{k^2}{M_{\mathbf{B}_c}} g_3(k^2) \right), \end{aligned} \quad (4)$$

where  $K_\pm = (M_{\mathbf{B}_c} \pm M_{\mathbf{B}_n})^2 - k^2$ .

The differential decay widths and asymmetries can be expressed in the following analytic forms in terms of the helicity amplitudes with the nonvanishing lepton masses of  $m_\ell$  [19],

$$\frac{d\Gamma}{dk^2} = \frac{1}{3} \frac{G_F^2}{(2\pi)^3} |V_{qc}|^2 \frac{(k^2 - m_\ell^2)^2 p}{8M_{\mathbf{B}_c}^2 k^2} \left[ \left( 1 + \frac{m_\ell^2}{2k^2} \right) \left( |H_{\frac{1}{2}1}|^2 + |H_{-\frac{1}{2}1}|^2 + |H_{\frac{3}{2}0}|^2 + |H_{-\frac{3}{2}0}|^2 \right) + \frac{3m_\ell^2}{2k^2} \left( |H_{\frac{1}{2}1}|^2 + |H_{-\frac{1}{2}1}|^2 \right) \right], \quad (5)$$

$$\langle \alpha(k^2) \rangle = \frac{\int dk^2 \frac{(k^2 - m_\ell^2)^2 p}{8M_{\mathbf{B}_c}^2 k^2} \left[ \left( 1 + \frac{m_\ell^2}{2k^2} \right) (|H_{\frac{1}{2}1}|^2 - |H_{-\frac{1}{2}1}|^2 + |H_{\frac{3}{2}0}|^2 - |H_{-\frac{3}{2}0}|^2) + \frac{3m_\ell^2}{2k^2} (|H_{\frac{1}{2}1}|^2 - |H_{-\frac{1}{2}1}|^2) \right]}{\int dk^2 \frac{(k^2 - m_\ell^2)^2 p}{8M_{\mathbf{B}_c}^2 k^2} \left[ \left( 1 + \frac{m_\ell^2}{2k^2} \right) (|H_{\frac{1}{2}1}|^2 + |H_{-\frac{1}{2}1}|^2 + |H_{\frac{3}{2}0}|^2 + |H_{-\frac{3}{2}0}|^2) + \frac{3m_\ell^2}{2k^2} (|H_{\frac{1}{2}1}|^2 + |H_{-\frac{1}{2}1}|^2) \right]}, \quad (6)$$

where  $p = \sqrt{K_+ K_-} / 2M_{\mathbf{B}_c}$  and  $H_{\lambda_2 \lambda_W} = H_{\lambda_2 \lambda_W}^V - H_{\lambda_2 \lambda_W}^A$ .

### B. Light front constituent quark model

From Eqs. (5) and (6), we see that as long as the timelike form factors are known, both branching ratios and averaged decay asymmetries can be determined. To calculate these timelike form factors, we use LFCQM, in which a baryon is treated as a bound state of three constituent quarks quantized in the LF formalism and its state is denoted by the momentum  $P$ , canonical spin  $S$ , and the  $z$ -direction projection of spin  $S_z$ , respectively. As a result, the baryon state can be expressed by [35,36,39,47–49]

$$|B, P, S, S_z\rangle = \int \{d^3\tilde{p}\} 2(2\pi)^3 \frac{1}{\sqrt{P^+}} \delta^3(\tilde{P} - \tilde{p}_1 - \tilde{p}_2 - \tilde{p}_3) \\ \times \sum_{\lambda_1, \lambda_2, \lambda_3} \Psi^{SS_z}(\tilde{p}_1, \tilde{p}_2, \tilde{p}_3, \lambda_1, \lambda_2, \lambda_3) \\ \times C^{\alpha\beta\gamma} F_{abc} |q_\alpha^a(\tilde{p}_1, \lambda_1) q_\beta^b(\tilde{p}_2, \lambda_2) q_\gamma^c(\tilde{p}_3, \lambda_3)\rangle, \quad (7)$$

where  $\Psi^{SS_z}(\tilde{p}_1, \tilde{p}_2, \tilde{p}_3, \lambda_1, \lambda_2, \lambda_3)$  is the vertex function describing the overlapping between the baryon and its constituents, which can be formally solved from the three-body Bethe-Salpeter equations,  $C^{\alpha\beta\gamma}$  ( $F_{abc}$ ) are the color (flavor) factors,  $\lambda_i$  and  $\tilde{p}_i$  with  $i = 1, 2, 3$  are the LF helicities and three momenta of the on-mass-shell constituent quarks, defined as

$$\tilde{p}_i = (p_i^+, p_{i\perp}), \quad p_{i\perp} = (p_i^1, p_i^2), \quad p_i^- = \frac{m_i^2 + p_{i\perp}^2}{p_i^+}, \quad (8)$$

and  $|q_\alpha^a(\tilde{p}, \lambda)\rangle$  and  $\{d^3\tilde{p}\}$  correspond to the light front constituent quark states and the integral measure, given by

$$|q_\alpha^a(\tilde{p}, \lambda)\rangle = d_\alpha^{i'a}(\tilde{p}, \lambda)|0\rangle, \quad \{d^3\tilde{p}\} \equiv \prod_{i=1,2,3} \frac{dp_i^+ d^2p_{i\perp}}{2(2\pi)^3}, \quad (9)$$

respectively, with the quark field operators satisfied the following anticommutation relations

$$\{d_\alpha^{i'a}(\tilde{p}', \lambda'), d_\alpha^{i'a}(\tilde{p}, \lambda)\} = 2(2\pi)^3 \delta^3(\tilde{p}' - \tilde{p}) \delta_{\lambda'\lambda} \delta_{\alpha\alpha'} \delta^{a'a}, \\ \delta^3(\tilde{p}) = \delta(p^+) \delta^2(p_\perp). \quad (10)$$

To separate the internal motion of the constituents from the bulk motion, we use the kinematic variables of  $(q_\perp, \xi)$ ,  $(Q_\perp, \eta)$ , and  $P_{\text{tot}}$ , given by

$$P_{\text{tot}} = \tilde{P}_1 + \tilde{P}_2 + \tilde{P}_3, \quad \xi = \frac{p_1^+}{p_1^+ + p_2^+}, \quad \eta = \frac{p_1^+ + p_2^+}{P_{\text{tot}}^+}, \\ q_\perp = (1 - \xi)p_{1\perp} - \xi p_{2\perp}, \quad Q_\perp = (1 - \eta)(p_{1\perp} + p_{2\perp}) - \eta p_{3\perp}, \quad (11)$$

where  $(q_\perp, \xi)$  and  $(Q_\perp, \eta)$  capture the relative motions between the first and second quarks, and the third and other two quarks, respectively. We consider the three constituent quarks in the baryon independently with suitable spin-flavor structures satisfying the Fermi statistics to have a correct baryon bound state system. The vertex function of  $\Psi^{SS_z}(\tilde{p}_1, \tilde{p}_2, \tilde{p}_3, \lambda_1, \lambda_2, \lambda_3)$  in Eq. (7) can be further written into two parts [35,36,50],

$$\Psi^{SS_z}(\tilde{p}_1, \tilde{p}_2, \tilde{p}_3, \lambda_1, \lambda_2, \lambda_3) = \phi(q_\perp, \xi, Q_\perp, \eta) \Xi^{SS_z}(\lambda_1, \lambda_2, \lambda_3), \quad (12)$$

where  $\phi(q_\perp, \xi, Q_\perp, \eta)$  is the momentum distribution of constituent quarks and  $\Xi^{SS_z}(\lambda_1, \lambda_2, \lambda_3)$  represents the momentum-dependent spin wave function, given by

$$\Xi^{SS_z}(\lambda_1, \lambda_2, \lambda_3) = \sum_{s_1, s_2, s_3} \langle \lambda_1 | R_1^\dagger | s_1 \rangle \langle \lambda_2 | R_2^\dagger | s_2 \rangle \langle \lambda_3 | R_3^\dagger | s_3 \rangle \\ \times \left\langle \frac{1}{2} s_1, \frac{1}{2} s_2, \frac{1}{2} s_3 | SS_z \right\rangle, \quad (13)$$

with the  $SU(2)$  Clebsch-Gordan coefficients of  $\langle \frac{1}{2} s_1, \frac{1}{2} s_2, \frac{1}{2} s_3 | SS_z \rangle$ , and  $R_i$  is the Melosh transformation matrix [36,51], which corresponds to the  $i$ th constituent quark, expressed by

$$R_M(x, p_\perp, m, M) = \frac{m + xM - i\vec{\sigma} \cdot (\vec{n} \times \vec{q})}{\sqrt{(m + xM)^2 + q_\perp^2}}, \\ R_1 = R_M(\eta, Q_\perp, M_3, M) R_M(\xi, q_\perp, m_1, M_3), \\ R_2 = R_M(\eta, Q_\perp, M_3, M) R_M(1 - \xi, -q_\perp, m_2, M_3), \\ R_3 = R_M(1 - \eta, -Q_\perp, m_3, M). \quad (14)$$

Here,  $\vec{\sigma}$  stands for the Pauli matrix,  $\vec{n} = (0, 0, 1)$ , and  $M$  and  $M_3$  are invariant masses of  $(q_\perp, \xi)$  and  $(Q_\perp, \eta)$  systems, represented by [36]

$$M_3^2 = \frac{q_\perp^2}{\xi(1 - \xi)} + \frac{m_1^2}{\xi} + \frac{m_2^2}{1 - \xi}, \\ M^2 = \frac{Q_\perp^2}{\eta(1 - \eta)} + \frac{M_3^2}{\eta} + \frac{m_3^2}{1 - \eta}, \quad (15)$$

respectively.

The spin-flavor structures of  $\mathbf{B}_c$  and  $\mathbf{B}_n$  are given by

$$\begin{aligned}
|\mathbf{B}_c\rangle &= \frac{1}{\sqrt{6}} [\phi_3 \chi^{\rho 3} (|q_1 q_2 c\rangle - |q_2 q_1 c\rangle) + \phi_2 \chi^{\rho 2} (|q_1 c q_2\rangle - |q_2 c q_1\rangle) + \phi_1 \chi^{\rho 1} (|c q_1 q_2\rangle - |c q_2 q_1\rangle)], \\
|\Lambda^0\rangle &= \frac{1}{\sqrt{6}} \phi [\chi^{\rho 3} (|dus\rangle - |uds\rangle) + \chi^{\rho 2} (|dsu\rangle - |usd\rangle) + \chi^{\rho 1} (|sdu\rangle - |sud\rangle)], \\
|\Sigma^0\rangle &= \frac{1}{\sqrt{6}} \phi [\chi^{\lambda 3} (|dus\rangle + |uds\rangle) + \chi^{\lambda 2} (|dsu\rangle + |usd\rangle) + \chi^{\lambda 1} (|sdu\rangle + |sud\rangle)], \\
|\mathbf{B}_n\rangle &= \frac{1}{\sqrt{3}} \phi [\chi^{\lambda 3} |q_1 q_1 q_2\rangle + \chi^{\lambda 2} |q_1 q_2 q_1\rangle + \chi^{\lambda 1} |q_2 q_1 q_1\rangle], \tag{16}
\end{aligned}$$

where  $q_{1(2)} = u, d, s$ ,  $B_n = (N, \Xi, \Sigma^+, \Sigma^-)$ ,  $\phi_{(i)}$  is the momentum distribution of the constituents with the corresponding spin-flavor configuration, and

$$\begin{aligned}
\chi_{\uparrow}^{\rho 3} &= \frac{1}{\sqrt{2}} (|\uparrow\downarrow\uparrow\rangle - |\downarrow\uparrow\uparrow\rangle), \\
\chi_{\uparrow}^{\lambda 3} &= \frac{1}{\sqrt{6}} (|\uparrow\downarrow\uparrow\rangle + |\downarrow\uparrow\uparrow\rangle - 2|\uparrow\uparrow\downarrow\rangle), \tag{17}
\end{aligned}$$

In principle, one could solve  $\phi_{(i)}$  from the Bethe-Salpeter equation with an explicit QCD-inspired potential, but it is beyond the scope of this paper. Nonetheless, we use a Gaussian type distribution with the phenomenological shape parameters  $\beta_Q$  and  $\beta_q$  to describe the relative motions of constituents. Consequently, we represent the LF kinematic variables  $(\xi, q_{\perp})$  and  $(\eta, Q_{\perp})$  in the forms of ordinary three momenta  $\mathbf{q} = (q_{\perp}, q_z)$  and  $\mathbf{Q} = (Q_{\perp}, Q_z)$ :

$$\begin{aligned}
\phi &= \mathcal{N} \sqrt{\frac{\partial q_z}{\partial \xi} \frac{\partial Q_z}{\partial \eta}} e^{-\frac{\mathbf{q}^2}{2\beta_q^2} - \frac{Q_z^2}{2\beta_Q^2}}, \\
q_z &= \frac{\xi M_3}{2} - \frac{m_1^2 + q_{\perp}^2}{2M_3 \xi}, \quad Q_z = \frac{\eta M}{2} - \frac{M_3^2 + Q_{\perp}^2}{2M \eta}, \tag{18}
\end{aligned}$$

where  $\mathcal{N}$  is the normalization constant. Since the one-particle baryonic state is normalized as

$$\langle \mathbf{B}, P', S', S'_z | \mathbf{B}, P, S, S_z \rangle = 2(2\pi)^3 P^+ \delta^3(\tilde{P}' - \tilde{P}) \delta_{S'_z S_z}, \tag{19}$$

the normalization condition of the momentum wave function is given by

$$\frac{1}{2^2(2\pi)^6} \int d\xi d\eta d^2 q_{\perp} d^2 Q_{\perp} |\phi_{(3)}|^2 = 1. \tag{20}$$

In this paper, we take different shape parameters of  $\beta_q$  and  $\beta_Q$  in the momentum wave functions  $\phi_i$  to describe the scalar diquark effects in  $\mathbf{B}_c$ . On the other hand, we assume the momentum-distribution function  $\phi$  of octet baryons  $\mathbf{B}_n$  is flavor symmetric for all constituents. In other words, the

$SU(3)_f$  flavor symmetry is held in the momentum wave function of  $\mathbf{B}_n$ . As a result, the shape parameters of  $\phi$  are equal, i.e.,  $\beta_{Q\mathbf{B}_n} = \beta_{q\mathbf{B}_n} = \beta_{\mathbf{B}_n}$ . Note that there is no  $SU(6)$  spin-flavor symmetry in  $\mathbf{B}_c$  and  $\mathbf{B}_n$  because of the momentum-dependent Melosh transformation even though the forms of these states are similar to those with the  $SU(6)$  spin-flavor wave functions.

### C. Transition form factors

We pick the  $\bar{q}\gamma^+(1-\gamma_5)c$  current or so-called good component of the baryon transition amplitudes

$$\begin{aligned}
&\langle \mathbf{B}_n, p_f, S'_z | \bar{q}\gamma^+(1-\gamma_5)c | \mathbf{B}_c, p_i, S_z \rangle \\
&= \bar{u}_{\mathbf{B}_n}(p_f, S'_z) \left[ \gamma^+ f_1(k^2) - i\sigma^{+\nu} \frac{k_{\nu}}{M_{\mathbf{B}_c}} f_2(k^2) + f_3(k^2) \frac{k^+}{M_{\mathbf{B}_c}} \right] \\
&\quad \times u_{\mathbf{B}_c}(p_i, S_z) \\
&\quad - \bar{u}_{\mathbf{B}_n}(p_f, S'_z) \left[ \gamma^+ g_1(k^2) - i\sigma^{+\nu} \frac{k_{\nu}}{M_{\mathbf{B}_c}} g_2(k^2) + g_3(k^2) \frac{k^+}{M_{\mathbf{B}_c}} \right] \\
&\quad \times \gamma_5 u_{\mathbf{B}_c}(p_i, S_z), \tag{21}
\end{aligned}$$

and choose the frame such that  $p_{i(f)}^+$  is conserved ( $k^+ = 0$ ,  $k^2 = -k_{\perp}^2$ ) to calculate the form factors to avoid zero-mode contributions and other  $x^+$ -ordered diagrams in the LF formalism [35,36]. The matrix elements of the vector and axial-vector currents at quark level correspond to three different lowest-order Feynman diagrams as shown in Fig. 1. Since the spin-flavor-momentum wave functions of baryons are totally symmetric under the permutation of constituents, we have that  $(a) + (b) + (c) = 3(a) = 3(b) = 3(c)$  [36]. We only present the calculation for the diagram (c), which contains simpler and cleaner forms with our notation  $(q_{\perp}, Q_{\perp}, \xi, \eta)$  as a demonstration. We can extract the form factors from the matrix elements through the relations

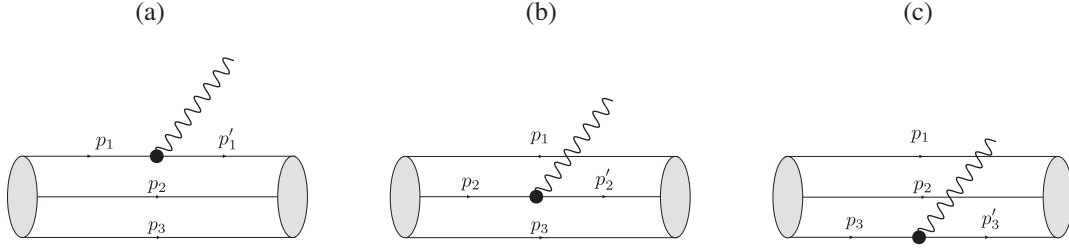


FIG. 1. Feynman diagrams for the baryonic weak transitions at the lowest order, where the sign of “filled circle” denotes the V-A current vertex, where (a)  $p'_1 - p_1 = k$ , (b)  $p'_2 - p_2 = k$ , and (c)  $p'_3 - p_3 = k$ .

$$\begin{aligned}
 f_1(k^2) &= \frac{1}{2p_i^+} \langle \mathbf{B}_n, p_f, \uparrow | \bar{q} \gamma^+ c | \mathbf{B}_c, p_i, \uparrow \rangle, \\
 f_2(k^2) &= \frac{1}{2p_i^+} \frac{M_{\mathbf{B}_c}}{k_\perp} \langle \mathbf{B}_n, p_f, \uparrow | \bar{q} \gamma^+ c | \mathbf{B}_c, p_i, \downarrow \rangle, \\
 g_1(k^2) &= \frac{1}{2p_i^+} \langle \mathbf{B}_n, p_f, \uparrow | \bar{q} \gamma^+ \gamma_5 c | \mathbf{B}_c, p_i, \uparrow \rangle, \\
 g_2(k^2) &= \frac{1}{2p_i^+} \frac{M_{\mathbf{B}_c}}{k_\perp} \langle \mathbf{B}_n, p_f, \uparrow | \bar{q} \gamma^+ \gamma_5 c | \mathbf{B}_c, p_i, \downarrow \rangle. \quad (22)
 \end{aligned}$$

Note that  $f_3$  and  $g_3$  are not available when  $k^+ = 0$ , but they are negligible because of the suppressions of  $k^2/M_{\mathbf{B}_c}^2$ . In fact,  $f_3$  and  $g_3$  are only associated with  $H_{\frac{1}{2}^+}^{V(A)}$ , which do not contribute to the semileptonic decays in the massless lepton limit [19]. As a result, we can safely set both  $f_3$  and  $g_3$  to be 0 in this study. With the help of the momentum distribution functions and Melosh transformation matrix in Eq. (7), the transition matrix elements can be written as

$$\begin{aligned}
 &\langle \mathbf{B}_n, p_f, S'_z | \bar{q} \gamma^+ (\gamma^5) c | \mathbf{B}_c, p_i, S_z \rangle \\
 &= \frac{1}{2^2 (2\pi)^6} \int d\xi d\eta d^2 q_\perp d^2 Q_\perp \phi(q'_\perp, \xi, Q'_\perp, \eta) \phi_3(q_\perp, \xi, Q_\perp, \eta) F^{lmn} F_{ijk} \delta_i^l \delta_m^j \\
 &\quad \times \sum_{s_1, s_2, s_3} \sum_{s'_1, s'_2, s'_3} \langle S', S'_z | s'_1, s'_2, s'_3 \rangle \langle s_1, s_2, s_3 | S, S_z \rangle \langle s'_1 | R'_1 R_1^\dagger | s_1 \rangle \langle s'_2 | R'_2 R_2^\dagger | s_2 \rangle \\
 &\quad \times 2P^+ (3\delta_n^q \delta_c^k) \langle s'_3 | R'_3 \sum_{\lambda'_3 \lambda_3} (\delta_{\lambda'_3}^{\lambda_3} ([\sigma_z]_{\lambda'_3}^{\lambda_3}) | \lambda'_3 \rangle \langle \lambda_3 |) R_3^\dagger | s_3 \rangle, \quad (23)
 \end{aligned}$$

where the indices of  $q$  and  $c$  in the delta symbols correspond to the quark flavors in the  $\bar{q} \gamma^+ (\gamma^5) c$  current,  $q'_\perp = q_\perp$  and  $Q'_\perp = Q_\perp + k_\perp$ . Using Eqs. (22) and (23), we find that

$$\begin{aligned}
 f_1(k^2) &= \frac{3}{2^2 (2\pi)^6} \int d\xi d\eta d^2 q_\perp d^2 Q_\perp \phi(q'_\perp, \xi, Q'_\perp, \eta) \phi_3(q_\perp, \xi, Q_\perp, \eta) (F^{lmn} F_{ijk} \delta_n^q \delta_c^k \delta_i^l \delta_m^j) \\
 &\quad \times \sum_{s_1, s_2, s_3} \sum_{s'_1, s'_2, s'_3} \langle S', \uparrow | s'_1, s'_2, s'_3 \rangle \langle s_1, s_2, s_3 | S, \uparrow \rangle \prod_{i=1,2,3} \langle s'_i | R'_i R_i^\dagger | s_i \rangle, \quad (24)
 \end{aligned}$$

$$\begin{aligned}
 g_1(k^2) &= \frac{3}{2^2 (2\pi)^6} \int d\xi d\eta d^2 q_\perp d^2 Q_\perp \phi(q'_\perp, \xi, Q'_\perp, \eta) \phi_3(q_\perp, \xi, Q_\perp, \eta) (F^{lmn} F_{ijk} \delta_n^q \delta_c^k \delta_i^l \delta_m^j) \\
 &\quad \times \sum_{s_1, s_2, s_3} \sum_{s'_1, s'_2, s'_3} \langle S', \uparrow | s'_1, s'_2, s'_3 \rangle \langle s_1, s_2, s_3 | S, \uparrow \rangle \prod_{i=1,2} \langle s'_i | R'_i R_i^\dagger | s_i \rangle \langle s'_3 | R'_3 \sigma_z R_3^\dagger | s_3 \rangle, \quad (25)
 \end{aligned}$$

$$\begin{aligned}
 f_2(k^2) &= \frac{3}{2^2 (2\pi)^6} \frac{M_{\mathbf{B}_c}}{k_\perp} \int d\xi d\eta d^2 q_\perp d^2 Q_\perp \phi(q'_\perp, \xi, Q'_\perp, \eta) \phi_3(q_\perp, \xi, Q_\perp, \eta) (F^{lmn} F_{ijk} \delta_n^q \delta_c^k \delta_i^l \delta_m^j) \\
 &\quad \times \sum_{s_1, s_2, s_3} \sum_{s'_1, s'_2, s'_3} \langle S', \uparrow | s'_1, s'_2, s'_3 \rangle \langle s_1, s_2, s_3 | S, \downarrow \rangle \prod_{i=1,2,3} \langle s'_i | R'_i R_i^\dagger | s_i \rangle, \quad (26)
 \end{aligned}$$

$$\begin{aligned}
 g_2(k^2) &= \frac{3}{2^2 (2\pi)^6} \frac{M_{\mathbf{B}_c}}{k_\perp} \int d\xi d\eta d^2 q_\perp d^2 Q_\perp \phi(q'_\perp, \xi, Q'_\perp, \eta) \phi_3(q_\perp, \xi, Q_\perp, \eta) (F^{lmn} F_{ijk} \delta_n^q \delta_c^k \delta_i^l \delta_m^j) \\
 &\quad \times \sum_{s_1, s_2, s_3} \sum_{s'_1, s'_2, s'_3} \langle S', \uparrow | s'_1, s'_2, s'_3 \rangle \langle s_1, s_2, s_3 | S, \downarrow \rangle \prod_{i=1,2} \langle s'_i | R'_i R_i^\dagger | s_i \rangle \langle s'_3 | R'_3 \sigma_z R_3^\dagger | s_3 \rangle. \quad (27)
 \end{aligned}$$

### III. NUMERICAL RESULTS

To find out the decay branching ratios and averaged asymmetries in the helicity formalism, we first calculate the transition form factors with LFCQM. By imposing the condition  $k^+ = 0$ , the form factors can be evaluated only in the spacelike region ( $k^2 = -k_\perp^2$ ) instead of the timelike one. Nonetheless, we still can extract the timelike information of the form factors via analytically continuations [39,48,52,53].

We fit  $f_{1(2)}(k^2)$  and  $g_{1(2)}(k^2)$  with the analytic functions in the spacelike region with the following form

$$F(k^2) = \frac{F(0)}{1 - q_1 k^2 + q_2 k^4}. \quad (28)$$

We employ the numerical values of the constituent quark masses and shape parameters in Table I. The values of the shape parameters can be determined approximately by the calculations in the mesonic cases [47,54]. Because the strength of the quark-quark pairs is a half of the quark-antiquark one [47], we will get the shape parameters of the quark pairs, which are approximately  $\sqrt{2}$  smaller than those in the mesonic cases.

We adopt  $\beta_{q\Lambda_c} \simeq 2(\beta_{u\bar{d}}/\sqrt{2})$  and  $\beta_{q\Xi_c} \simeq 2(\beta_{s\bar{u}(\bar{d})}/\sqrt{2})$ , where the factor of 2 comes from the effects of the diquark clustering, making the light quark pairs to be more compact in  $\mathbf{B}_c$  baryons. For the octet baryons of  $\mathbf{B}_n$ , we assume that the  $SU(3)_f$  flavor symmetry is hold, and therefore, the shape parameters is flavor symmetric for each constituent, i.e.,  $\beta_Q = \beta_q$ . As a result, we approximate the shape parameters of the octet baryons equal to the mesonic ones by effectively treating any pair of two constituents as a heavier antiquark. By using Eqs. (24)–(27), we numerically compute 32 points for all form factors from  $k^2 = 0$  to  $k^2 = -9.7 \text{ GeV}^2$  and fit them with the MATLAB curve fitting toolbox. We present our fitting results of the form factors in Tables II–IV, and our predictions of the branching ratios and asymmetry parameters in Table V. The comparisons with different theoretical models are presented in Tables VI–VIII.

The uncertainties of our results mainly arise from the extrapolations by the analytical continuation method. The magnitudes of average asymmetry parameters predicted by

TABLE I. Values of the constituent quark masses ( $m_i$ ) and shape parameters ( $\beta_{q\mathbf{B}_c}$ ,  $\beta_{Q\mathbf{B}_c}$ ,  $\beta_{\mathbf{B}_n}$ ) in units of GeV.

$m_c$	$m_s$	$m_d$	$m_c$	$\beta_{q\Lambda_c}$	$\beta_{Q\Lambda_c}$
1.3	0.4	0.26	0.26	0.44	0.53
$\beta_{q\Xi_c}$	$\beta_{Q\Xi_c}$	$\beta_N$	$\beta_\Lambda$	$\beta_\Sigma$	$\beta_\Xi$
0.49	0.53	0.32	0.34	0.34	0.37

TABLE II. Fitting results of the  $\Lambda_c^+ \rightarrow \mathbf{B}_n$  form factors in LFCQM.

$\Lambda_c^+ \rightarrow \Lambda$				
	$f_1$	$f_2$	$g_1$	$g_2$
$F(0)$	$0.67 \pm 0.01$	$0.76 \pm 0.02$	$0.59 \pm 0.01$	$(3.8 \pm 1.2) \times 10^{-3}$
$q_1$	$1.48 \pm 0.31$	$1.44 \pm 0.30$	$1.22 \pm 0.28$	$4.99 \pm 17.6$
$q_2$	$2.29 \pm 0.49$	$2.23 \pm 0.48$	$1.82 \pm 0.39$	$24.8 \pm 95.8$
$\Lambda_c^+ \rightarrow n$				
	$f_1$	$f_2$	$g_1$	$g_2$
$F(0)$	$0.83 \pm 0.01$	$1.05 \pm 0.02$	$0.71 \pm 0.01$	$0.27 \pm 0.01$
$q_1$	$1.25 \pm 0.36$	$1.20 \pm 0.30$	$0.94 \pm 0.28$	$1.37 \pm 0.40$
$q_2$	$1.85 \pm 0.68$	$1.78 \pm 0.48$	$1.36 \pm 0.39$	$2.08 \pm 0.83$

TABLE III. Fitting results of the  $\Xi_c^+ \rightarrow \mathbf{B}_n$  form factors in LFCQM.

$\Xi_c^+ \rightarrow \Xi^0$				
	$f_1$	$f_2$	$g_1$	$g_2$
$F(0)$	$0.77 \pm 0.02$	$0.96 \pm 0.02$	$0.69 \pm 0.01$	$(6.8 \pm 0.3) \times 10^{-3}$
$q_1$	$1.50 \pm 0.31$	$1.45 \pm 0.31$	$1.25 \pm 0.28$	$2.00 \pm 0.76$
$q_2$	$2.30 \pm 0.49$	$2.26 \pm 0.49$	$1.85 \pm 0.39$	$3.00 \pm 1.41$
$\Xi_c^+ \rightarrow \Sigma^0$				
	$f_1$	$f_2$	$g_1$	$g_2$
$F(0)$	$0.52 \pm 0.01$	$0.70 \pm 0.02$	$0.45 \pm 0.01$	$0.08 \pm 0.01$
$q_1$	$1.49 \pm 0.32$	$1.43 \pm 0.33$	$1.18 \pm 0.28$	$1.88 \pm 0.39$
$q_2$	$2.35 \pm 0.51$	$2.38 \pm 0.53$	$1.79 \pm 0.38$	$2.88 \pm 0.67$
$\Xi_c^+ \rightarrow \Lambda$				
	$f_1$	$f_2$	$g_1$	$g_2$
$F(0)$	$0.28 \pm 0.01$	$0.38 \pm 0.01$	$0.25 \pm 0.01$	$0.04 \pm 0.01$
$q_1$	$1.50 \pm 0.31$	$1.35 \pm 0.51$	$1.18 \pm 0.28$	$1.71 \pm 0.38$
$q_2$	$2.32 \pm 0.50$	$2.30 \pm 0.81$	$1.77 \pm 0.38$	$2.78 \pm 0.66$

TABLE IV. Fitting results of the  $\Xi_c^0 \rightarrow \mathbf{B}_n$  form factors in LFCQM.

$\Xi_c^0 \rightarrow \Xi^-$				
	$f_1$	$f_2$	$g_1$	$g_2$
$F(0)$	$0.74 \pm 0.02$	$0.96 \pm 0.02$	$0.69 \pm 0.01$	$(6.8 \pm 0.3) \times 10^{-3}$
$q_1$	$1.50 \pm 0.31$	$1.47 \pm 0.31$	$1.21 \pm 0.28$	$2.00 \pm 0.76$
$q_2$	$2.30 \pm 0.50$	$2.25 \pm 0.48$	$1.98 \pm 0.39$	$3.00 \pm 1.41$
$\Xi_c^0 \rightarrow \Sigma^-$				
	$f_1$	$f_2$	$g_1$	$g_2$
$F(0)$	$0.73 \pm 0.01$	$0.99 \pm 0.02$	$0.63 \pm 0.01$	$0.11 \pm 0.01$
$q_1$	$1.49 \pm 0.32$	$1.43 \pm 0.33$	$1.18 \pm 0.28$	$1.88 \pm 0.39$
$q_2$	$2.35 \pm 0.51$	$2.38 \pm 0.53$	$1.79 \pm 0.38$	$2.88 \pm 0.70$

TABLE V. Predictions of the decay branching ratios and asymmetry parameters.

	$\ell^+ = e^+$		$\ell^+ = \mu^+$	
	$\mathcal{B}(\%)$	$\alpha$	$\mathcal{B}(\%)$	$\alpha$
$\Lambda_c^+ \rightarrow \Lambda \ell^+ \nu_\ell$	$3.55 \pm 1.04$	$-0.97 \pm 0.03$	$3.40 \pm 1.02$	$-0.98 \pm 0.02$
$\Lambda_c^+ \rightarrow n \ell^+ \nu_\ell$	$0.36 \pm 0.15$	$-0.96 \pm 0.04$	$0.34 \pm 0.15$	$-0.96 \pm 0.04$
$\Xi_c^+ \rightarrow \Xi^0 \ell^+ \nu_\ell$	$11.3 \pm 3.35$	$-0.97 \pm 0.03$	$10.8 \pm 3.3$	$-0.97 \pm 0.03$
$\Xi_c^+ \rightarrow \Sigma^0 \ell^+ \nu_\ell$	$0.33 \pm 0.09$	$-0.98 \pm 0.01$	$0.31 \pm 0.09$	$-0.98 \pm 0.02$
$\Xi_c^+ \rightarrow \Lambda \ell^+ \nu_\ell$	$0.12 \pm 0.04$	$-0.98 \pm 0.02$	$0.11 \pm 0.05$	$-0.98 \pm 0.02$
$\Xi_c^0 \rightarrow \Xi^- \ell^+ \nu_\ell$	$3.49 \pm 0.95$	$-0.98 \pm 0.02$	$3.34 \pm 0.94$	$-0.98 \pm 0.02$
$\Xi_c^0 \rightarrow \Sigma^- \ell^+ \nu_\ell$	$0.22 \pm 0.06$	$-0.98 \pm 0.02$	$0.21 \pm 0.06$	$-0.98 \pm 0.02$

TABLE VI. Our results of  $\Lambda_c^+ \rightarrow \mathbf{B}_n e^+ \nu_e$  decay in comparison with the experimental data and those in various calculations in the literature.

	$\Lambda_c^+ \rightarrow \Lambda e^+ \nu_e$		$\Lambda_c^+ \rightarrow n e^+ \nu_e$	
	$\mathcal{B}(\%)$	$\alpha$	$\mathcal{B}(\%)$	$\alpha$
LFCQM	$3.55 \pm 1.04$	$-0.97 \pm 0.03$	$0.36 \pm 0.15$	$-0.96 \pm 0.04$
Data [4]	$3.6 \pm 0.4$	$-0.86 \pm 0.04$	...	...
$SU(3)$ [19]	$3.2 \pm 0.3$	$-0.86 \pm 0.04$	$0.51 \pm 0.04$	$-0.89 \pm 0.04$
RQM [28,29]	3.25	-0.86	0.268	-0.91
HQET [25]	1.42	...	...	...
LF [33]	1.63	...	0.201	...
MBM (NRQM) [34]	2.6 (3.2)	...	0.20 (0.30)	...
LQCD [26,27]	$3.80 \pm 0.22$	...	$0.41 \pm 0.03$	...
CCQM [30]	2.78	-0.87	0.20	...
LCSR [31,32]	$3.0 \pm 0.3$	...	$8.69 \pm 2.89$	...

TABLE VII. Our result of  $\Xi_c^+ \rightarrow \mathbf{B}_n e^+ \nu_e$  decays in comparison with the experimental data and those in various calculations in the literature.

	$\Xi_c^+ \rightarrow \Xi^0 e^+ \nu_e$		$\Xi_c^+ \rightarrow \Sigma^0 e^+ \nu_e$ $\Xi_c^+ \rightarrow \Lambda e^+ \nu_e$	
	$\mathcal{B}(\%)$	$\alpha$	$\mathcal{B}(\%)$	$\alpha$
LFCQM	$11.3 \pm 3.35$	$-0.97 \pm 0.03$	$0.33 \pm 0.09$	$-0.98 \pm 0.01$
Data [2,4]	$6.6^{+3.7}_{-3.5}$	...	$0.12 \pm 0.04$	$-0.98 \pm 0.02$
$SU(3)$ [19]	$10.7 \pm 0.9$	$-0.83 \pm 0.04$	...	...
RQM [29]	9.40	-0.80	$0.46 \pm 0.04$	$-0.85 \pm 0.04$
LF [33]	5.39	...	$0.22 \pm 0.02$	$-0.86 \pm 0.04$
MBM (NRQM) [34]	11.1 (13.3)	...	...	...
			0.13	-0.84
			0.19	...
			0.08	...
			0.28 (0.41)	...
			0.09 (0.14)	...

LFCQM almost reach their extremums in all channels. As shown in Tables VI–VIII, we obtain that  $\mathcal{B}(\Lambda_c^+ \rightarrow \Lambda e^+ \nu_e) = (3.55 \pm 1.04)\%$ ,  $\mathcal{B}(\Xi_c^+ \rightarrow \Xi^0 e^+ \nu_e) = (11.3 \pm 3.4)\%$ , and  $\mathcal{B}(\Xi_c^0 \rightarrow \Xi^- e^+ \nu_e) = (3.49 \pm 0.95)\%$ , which are all consistent with the current data from PDG [4] and the

BELLE experiments [1,2]. Our branching ratios are also consistent with the predictions of the relativistic quark model (RQM) [28,29], the covariant constituent quark model (CCQM) [30], and the  $SU(3)_F$  approach [19]. The results given by the LF formalism [33] and heavy quark effective

TABLE VIII. Our result of  $\Xi_c^0 \rightarrow \mathbf{B}_n e^+ \nu_e$  decays in comparison with the experimental data and those in various calculations in the literature.

	$\Xi_c^0 \rightarrow \Xi^- e^+ \nu_e$		$\Xi_c^0 \rightarrow \Sigma^- e^+ \nu_e$	
	$\mathcal{B}(\%)$	$\alpha$	$\mathcal{B}(\%)$	$\alpha$
LFCQM	$3.49 \pm 0.95$	$-0.98 \pm 0.03$	$0.22 \pm 0.06$	$-0.98 \pm 0.02$
Data [1,4]	$1.8 \pm 1.2$	...	...	...
$SU(3)$ [19]	$3.7 \pm 0.3$	$-0.83 \pm 0.04$	$0.33 \pm 0.03$	$-0.85 \pm 0.04$
RQM [29]	2.38	-0.80	...	...
LF [33]	1.35	...	0.10	...
MBM (NRQM) [34]	3.55 (4.47)	...	0.19 (0.26)	...

theory (HQET) [25] are half of ours because they choose the spin-flavor wave function of  $\mathbf{B}_c$  to be  $c(q_1 q_2 - q_2 q_1) \chi_{s_z}^{\rho_3}$  instead of the totally symmetric one. The averaged asymmetry parameter predicted by LFCQM in  $\Lambda_c^+ \rightarrow \Lambda e^+ \nu_e$  is 10% lower than the data. Since we do not consider any parameters about spin interactions in our phenomenological wave functions, the helicity-structure-related results, such as the decay asymmetries, are clearly not precise enough to explain the experimental data. On the other hand, the prediction from RQM and the  $SU(3)_f$  approach are almost the same as the data. Since the authors for RQM in Refs. [28,29] have considered a comprehensive QCD-inspired potential including the chromomagnetic effect, their results are more close to the experimental values than ours. Meanwhile, the  $SU(3)_f$  approach is a model independent way to analyze  $\mathbf{B}_c \rightarrow \mathbf{B}_n \ell^+ \nu_\ell$  decays, which automatically includes the information related to the spin interaction when the asymmetry parameters are used as the fitting inputs. Clearly, our results of the asymmetry parameters could be improved by considering the full QCD potential and its solutions.

#### IV. CONCLUSIONS

We have systematically studied the semileptonic decays of  $\mathbf{B}_c \rightarrow \mathbf{B}_n \ell^+ \nu_\ell$  in LFCQM. By requiring the constituents in the baryonic states to obey the Fermi statistics, we are able to determine the overall spin-flavor-momentum structures of the baryons. We assume that the momentum

distribution of  $\mathbf{B}_n$  is symmetric in flavor indices and any pair of two quarks can be effectively treated as a heavier antiquark. We have found that  $\mathcal{B}(\Lambda_c^+ \rightarrow \Lambda e^+ \nu_e) = (3.55 \pm 1.04)\%$ ,  $\mathcal{B}(\Xi_c^+ \rightarrow \Xi^0 e^+ \nu_e) = (11.3 \pm 3.35)\%$ , and  $\mathcal{B}(\Xi_c^0 \rightarrow \Xi^- e^+ \nu_e) = (3.49 \pm 0.95)\%$  in LFCQM: this is consistent with the experimental data of  $(3.6 \pm 0.4) \times 10^{-2}$  [4],  $(6.6_{-3.5}^{+3.7}) \times 10^{-2}$  [2,4] and  $(1.8 \pm 1.2) \times 10^{-2}$  [1,4] as well as the values predicted by  $SU(3)_F$  [19], LQCD [26,27], RQM [28], and CCQM [30], but twice larger than those in HQET [25] and LF [33]. We have also obtained that  $\alpha(\Lambda_c^+ \rightarrow \Lambda e^+ \nu_e) = (-0.97 \pm 0.03)$  in LFCQM, which is 10% lower than the experimental data of  $-0.86 \pm 0.04$  [4]. The reason of this deviation may arise from the QCD spin-spin interacting effects, which are not included in our phenomenological wave functions. Our results of the averaged decay asymmetries could be improved if we consider the wave function solved from the full QCD potential. It is clear that our predicted values for the decay branching ratios and asymmetries in  $\Xi_c^{+(0)} \rightarrow \mathbf{B}_n e^+ \nu_e$  could be tested in the ongoing experiments at LHCb and BELLEII.

#### ACKNOWLEDGMENTS

We would like to thank Professor Chengping Shen for discussions. This work was supported in part by National Center for Theoretical Sciences and MoST (Grant No. MoST-107-2119-M-007-013-MY3).

- 
- |   |   |
|---|---|
| <p>[1] Y. B. Li <i>et al.</i> (Belle Collaboration), <i>Phys. Rev. Lett.</i> <b>122</b>, 082001 (2019).</p> <p>[2] Y. B. Li <i>et al.</i> (Belle Collaboration), <i>Phys. Rev. D</i> <b>100</b>, 031101 (2019).</p> <p>[3] R. Aaij <i>et al.</i> (LHCb Collaboration), <i>Phys. Rev. D</i> <b>100</b>, 032001 (2019).</p> <p>[4] P. A. Zyla <i>et al.</i> (Particle Data Group), <i>Prog. Theor. Exp. Phys.</i> <b>2020</b>, 083C01 (2020).</p> | <p>[5] M. J. Savage and R. P. Springer, <i>Phys. Rev. D</i> <b>42</b>, 1527 (1990).</p> <p>[6] M. J. Savage, <i>Phys. Lett. B</i> <b>257</b>, 414 (1991).</p> <p>[7] C. D. Lu, W. Wang, and F. S. Yu, <i>Phys. Rev. D</i> <b>93</b>, 056008 (2016).</p> <p>[8] C. Q. Geng, Y. K. Hsiao, C. W. Liu, and T. H. Tsai, <i>J. High Energy Phys.</i> <b>11</b> (2017) 147.</p> <p>[9] W. Wang, Z. P. Xing, and J. Xu, <i>Eur. Phys. J. C</i> <b>77</b>, 800 (2017).</p> |
|---|---|

- [10] C. Q. Geng, Y. K. Hsiao, Y. H. Lin, and L. L. Liu, *Phys. Lett. B* **776**, 265 (2018).
- [11] C. Q. Geng, Y. K. Hsiao, C. W. Liu, and T. H. Tsai, *Phys. Rev. D* **97**, 073006 (2018); *Eur. Phys. J. C* **78**, 593 (2018).
- [12] D. Wang, P. F. Guo, W. H. Long, and F. S. Yu, *J. High Energy Phys.* 03 (2018) 066.
- [13] X. G. He and W. Wang, *Chin. Phys. C* **42**, 103108 (2018).
- [14] C. Q. Geng, Y. K. Hsiao, C. W. Liu, and T. H. Tsai, *Phys. Rev. D* **99**, 073003 (2019).
- [15] C. Q. Geng, C. W. Liu, and T. H. Tsai, *Phys. Lett. B* **790**, 225 (2019); **794**, 19 (2019).
- [16] C. Q. Geng, C. W. Liu, T. H. Tsai, and Y. Yu, *Phys. Rev. D* **99**, 114022 (2019).
- [17] J. Y. Cen, C. Q. Geng, C. W. Liu, and T. H. Tsai, *Eur. Phys. J. C* **79**, 946 (2019).
- [18] Y. K. Hsiao, Y. Yao, and H. J. Zhao, *Phys. Lett. B* **792**, 35 (2019).
- [19] C. Q. Geng, C. W. Liu, T. H. Tsai, and S. W. Yeh, *Phys. Lett. B* **792**, 214 (2019).
- [20] Y. Grossman and S. Schacht, *J. High Energy Phys.* 07 (2019) 020.
- [21] X. G. He, Y. J. Shi, and W. Wang, *Eur. Phys. J. C* **80**, 359 (2020).
- [22] S. Roy, R. Sinha, and N. G. Deshpande, *Phys. Rev. D* **101**, 036018 (2020).
- [23] C. Q. Geng, C. C. Lih, C. W. Liu, and T. H. Tsai, *Phys. Rev. D* **101**, 094017 (2020).
- [24] C. P. Jia, D. Wang, and F. S. Yu, *Nucl. Phys.* **B956**, 115048 (2020).
- [25] H. Y. Cheng and B. Tseng, *Phys. Rev. D* **53**, 1457 (1996).
- [26] S. Meinel, *Phys. Rev. Lett.* **118**, 082001 (2017).
- [27] S. Meinel, *Phys. Rev. D* **97**, 034511 (2018).
- [28] R. N. Faustov and V. O. Galkin, *Eur. Phys. J. C* **76**, 628 (2016).
- [29] R. N. Faustov and V. O. Galkin, *Eur. Phys. J. C* **79**, 695 (2019); *Particles* **3**, 208 (2020).
- [30] T. Gutsche, M. A. Ivanov, J. G. Korner, V. E. Lyubovitskij, and P. Santorelli, *Phys. Rev. D* **93**, 034008 (2016).
- [31] Y. L. Liu, M. Q. Huang, and D. W. Wang, *Phys. Rev. D* **80**, 074011 (2009).
- [32] K. Azizi, M. Bayar, Y. Sarac, and H. Sundu, *Phys. Rev. D* **80**, 096007 (2009).
- [33] Z. X. Zhao, *Chin. Phys. C* **42**, 093101 (2018).
- [34] R. Perez-Marcial, R. Huerta, A. Garcia, and M. Avila-Aoki, *Phys. Rev. D* **40**, 2955 (1989); **44**, 2203(E) (1991).
- [35] W. M. Zhang, *Chin. J. Phys.* **32**, 717 (1994).
- [36] F. Schlumpf, [arXiv:hep-ph/9211255](https://arxiv.org/abs/hep-ph/9211255).
- [37] C. Q. Geng, C. C. Lih, and W. M. Zhang, *Phys. Rev. D* **62**, 074017 (2000).
- [38] C. Q. Geng, C. W. Hwang, and C. C. Liu, *Phys. Rev. D* **65**, 094037 (2002).
- [39] H. Y. Cheng, C. K. Chua, and C. W. Hwang, *Phys. Rev. D* **70**, 034007 (2004).
- [40] C. Q. Geng, C. C. Lih, and C. Xia, *Eur. Phys. J. C* **76**, 313 (2016).
- [41] H. Y. Cheng and X. W. Kang, *Eur. Phys. J. C* **77**, 587 (2017); **77**, 863(E) (2017).
- [42] Z. X. Zhao, *Eur. Phys. J. C* **78**, 756 (2018).
- [43] Z. P. Xing and Z. X. Zhao, *Phys. Rev. D* **98**, 056002 (2018).
- [44] Q. Chang, L. T. Wang, and X. N. Li, *J. High Energy Phys.* 12 (2019) 102.
- [45] C. K. Chua, *Phys. Rev. D* **99**, 014023 (2019); **100**, 034025(E) (2019).
- [46] A. Kadeer, J. G. Korner, and U. Moosbrugger, *Eur. Phys. J. C* **59**, 27 (2009).
- [47] H. W. Ke, N. Hao, and X. Q. Li, *Eur. Phys. J. C* **79**, 540 (2019).
- [48] H. W. Ke, X. Q. Li, and Z. T. Wei, *Phys. Rev. D* **77**, 014020 (2008).
- [49] H. W. Ke, X. H. Yuan, X. Q. Li, Z. T. Wei, and Y. X. Zhang, *Phys. Rev. D* **86**, 114005 (2012).
- [50] C. Lorce, B. Pasquini, and M. Vanderhaeghen, *J. High Energy Phys.* 05 (2011) 041.
- [51] W. N. Polyzou, W. Glockle, and H. Witala, *Few Body Syst.* **54**, 1667 (2013).
- [52] W. Jaus, *Phys. Rev. D* **44**, 2851 (1991).
- [53] W. Jaus, *Phys. Rev. D* **53**, 1349 (1996); **54**, 5904(E) (1996).
- [54] Q. Chang, X. N. Li, X. Q. Li, F. Su, and Y. D. Yang, *Phys. Rev. D* **98**, 114018 (2018).